Indirect dark matter detection

Teresa Marrodán Undagoitia

- **Program**
  - Locations of indirect signals
  - Possible processes and signal rates: annihilation and decay
  - Particle propagation and detection

- **Literature:**
  - Louis E. Strigari, *Galactic searches for dark matter*, Phys. Rep. 531 (2013) 1
  - Marco Cirelli *et al.*, *PPPC 4 DM ID: A Poor Particle Physicist Cookbook for Dark Matter Indirect Detection*, JCAP 1103 (2011) 051 & arXiv:1012.4515
  - IceCube Collaboration, Phys. Rev. **88** (2013) 122001
  - J. Conrad *et al.*, *WIMP searches with gamma rays in the Fermi era: challenges, methods and results*, arXiv:1503.06348
  - Fermi-LAT Collaboration, *Searching for Dark Matter Annihilation from Milky Way Dwarf Spheroidal Galaxies with Six Years of Fermi Large Area Telescope Data*, PRL **115** (2015) 231301
  - D. Hooper and L. Goodenough, *Dark Matter Annihilation in The Galactic Center As Seen by the Fermi Gamma Ray Space Telescope*, Phys. Lett. B697 (2011) 412, arXiv:1010.2752
  - E. Bulbul *et al.*, *Detection of an unidentified emission line in the stated X-ray spectrum of galaxy clusters*, ApJ **789** (2014) 13
  - AMS Collaboration, Phys. Rev. Lett. **113** (2014) 121101

- **Material for the lecture:**

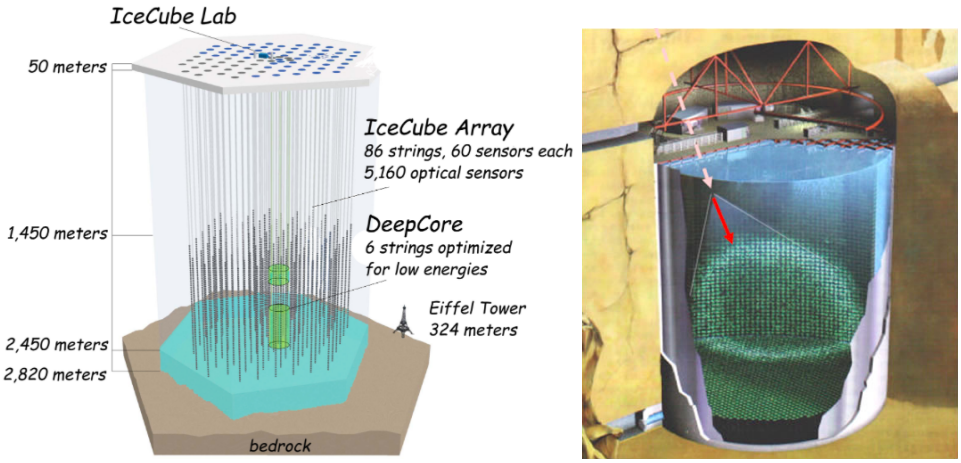

Figure 1: (Right) Schematics of the IceCube detector. Figure from *Into the Ice: Completing the IceCube Neutrino Observatory*, Berkeley Lab. (Left) Schematics of the SuperKamiokande detector. Figure from SuperKamiokande homepage.

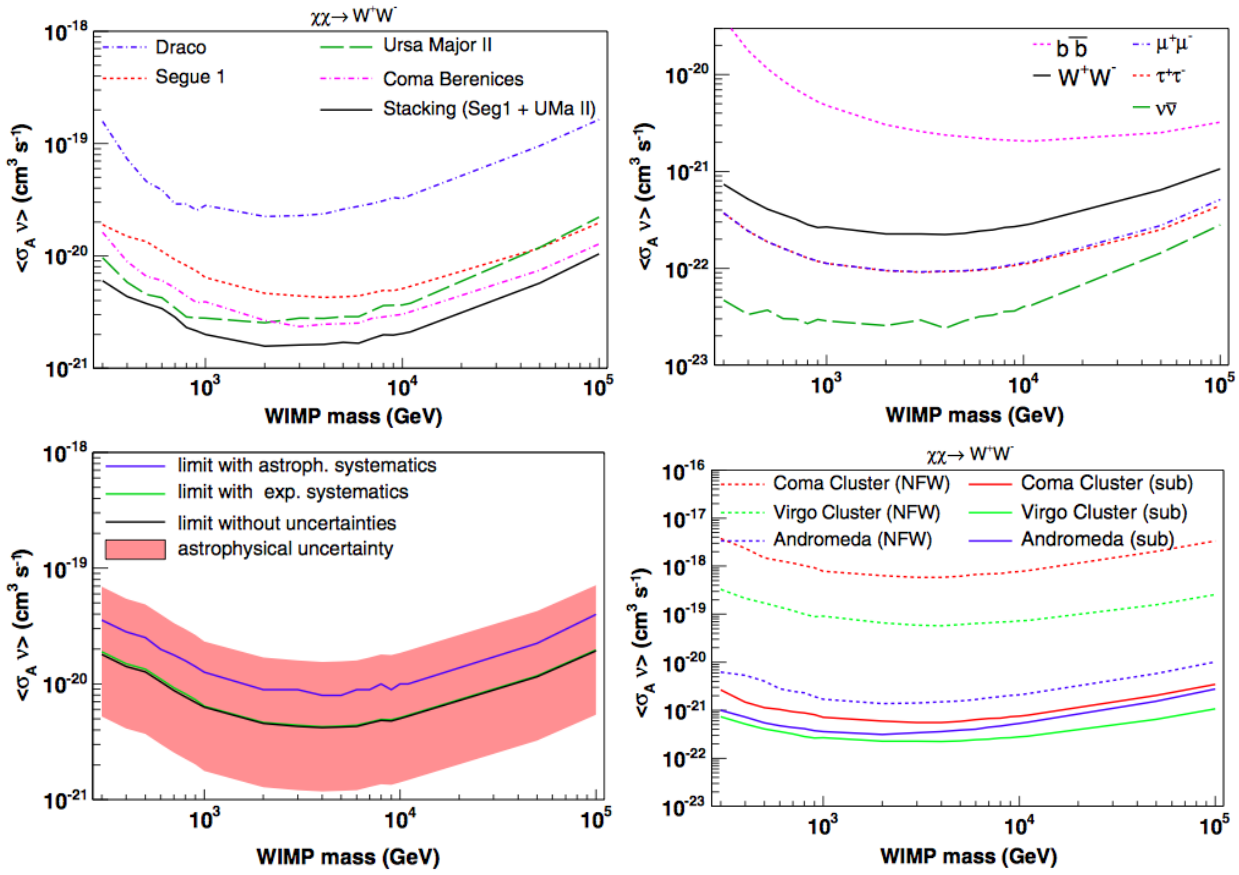

Figure 2: Ice Cube searches for self-annihilating dark matter in nearby galaxies and galaxy clusters. Top left: upper limits for annihilation into W^+W^- for dwarf galaxies. Top right: upper limits for the Virgo cluster for annihilation into $b\bar{b}$, W^+W^-, $\tau^+\tau^-$, $\mu^+\mu^-$, and $\nu\bar{\nu}$. Bottom left: upper limit for Segue 1 for annihilation into W^+W^- including astrophysical uncertainties. Bottom right: upper limits for the Coma and Virgo clusters and the Andromeda galaxy (W^+W^- annihilation) assuming a pure NFW profile (dashed) and taking into account substructures within halos (solid). Figures from IceCube collaboration, Phys. Rev. **88** (2013) 122001.

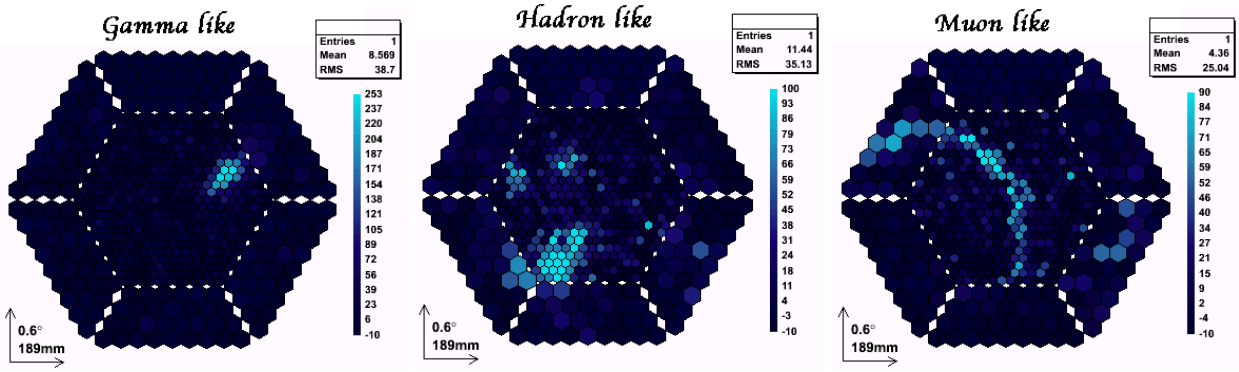

Figure 3: Examples of signals in one of the MAGIC Chrenkov telescopes. Figures from the MAGIC Collaboration (homepage).

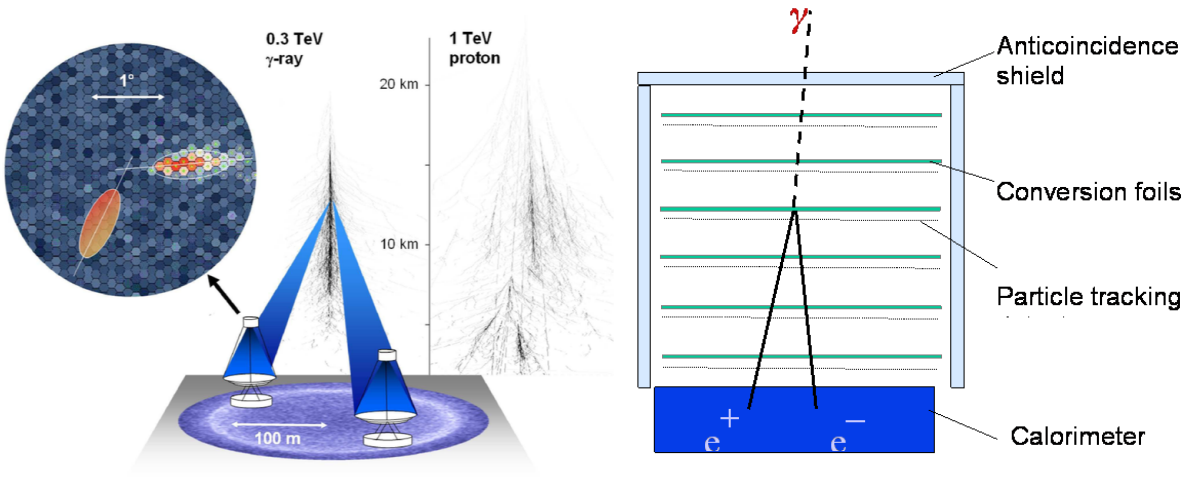

Figure 4: (Left) Imaging Cherenkov telescope. Figure from Hinton & Hofmann, Annu. Rev. Astrophys. 47 (2009) 523. (Right) Scheme of the the FermiLAT instrument from Fermi homepage.

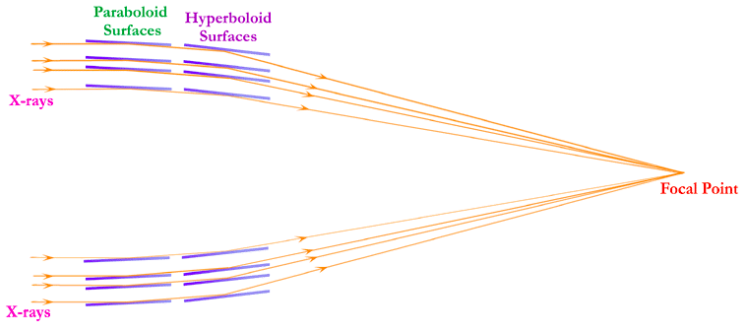

Figure 5: Schematic of grazing X-ray telescope illustrating the principle of grazing incidence reflection and focussing of X-rays. Figure from Chandra homepage.

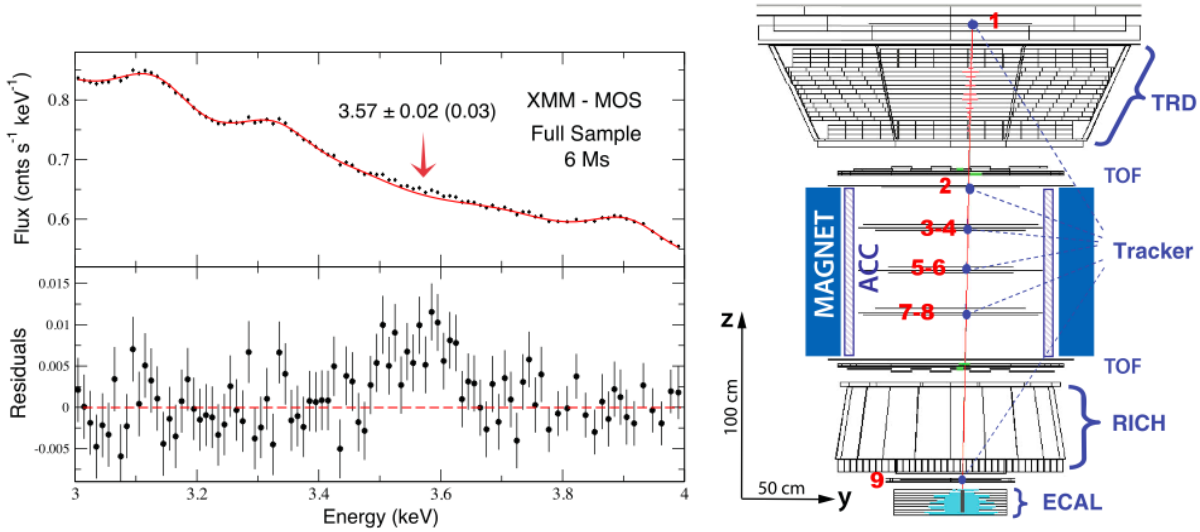

Figure 6: (Left) XMM-Newton data in the region $(3-4)$ keV stacking several galaxy clusters. Figure from E. Bulbul *et al.*, ApJ **789** (2014) 13. (Right) Schematics of AMS from the homepage.

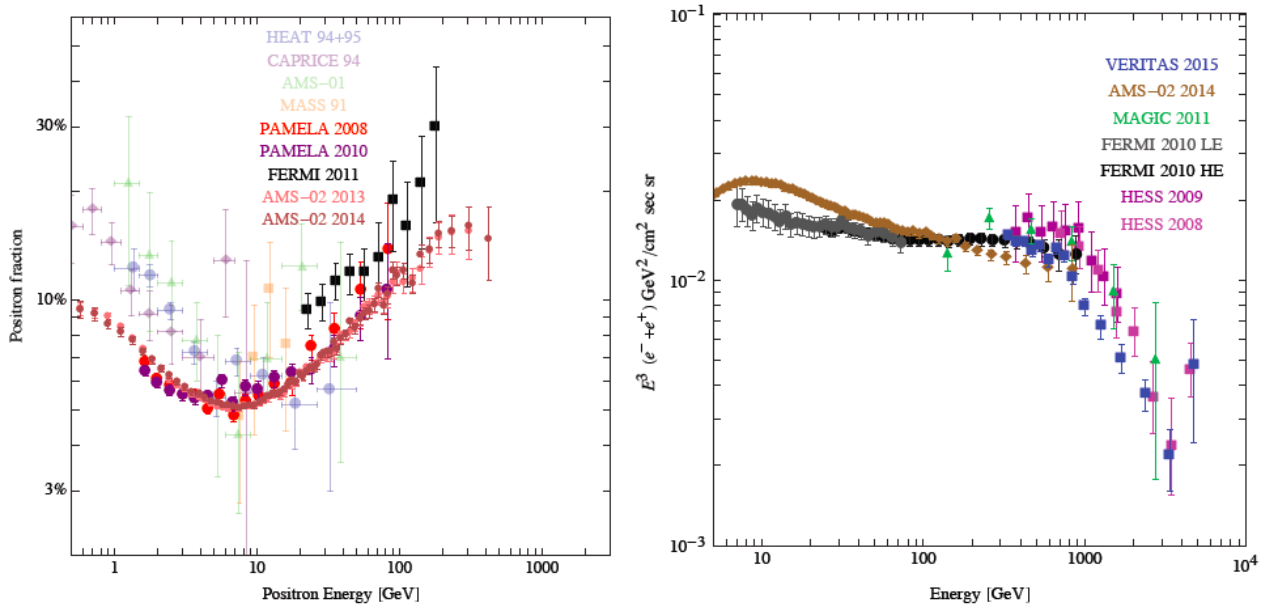

Figure 7: Compilation of data in charged cosmic rays: positron fraction (left) and sum of electrons and positrons (right). Figure from M. Cirelli (2015) arXiv:1511.02031.

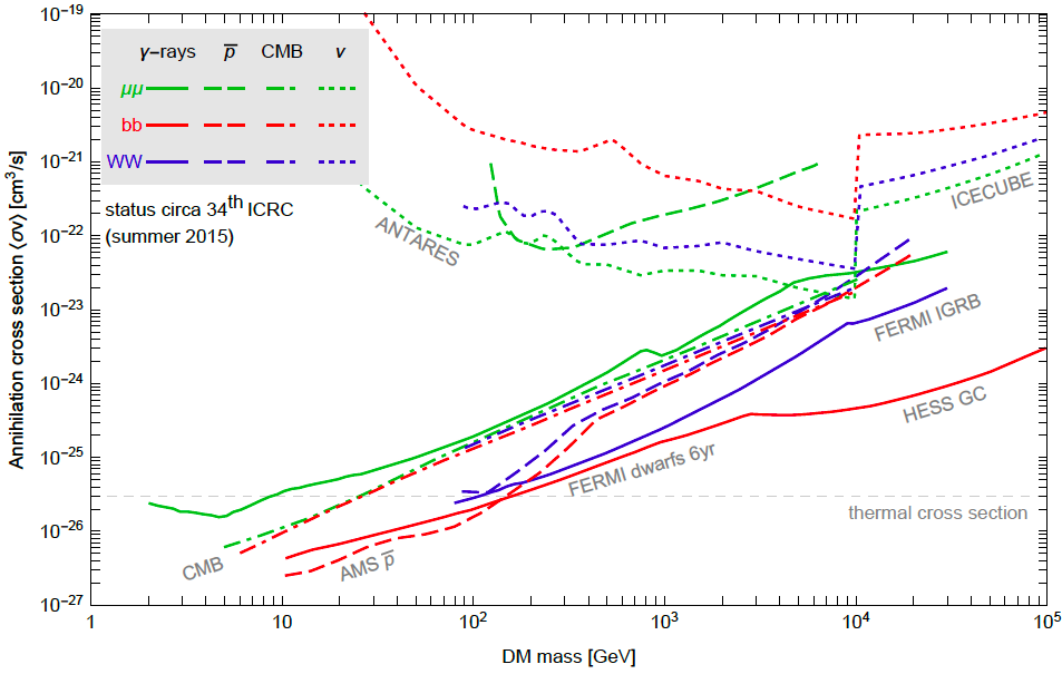

Figure 8: Summary figure of the current most stringent bounds on dark matter annihilation in different channels and from different searches. The data originates from AMS-02, Fermi, CMB, HESS, ANTARES and IceCube. Figure from M. Cirelli (2015) arXiv:1511.02031.